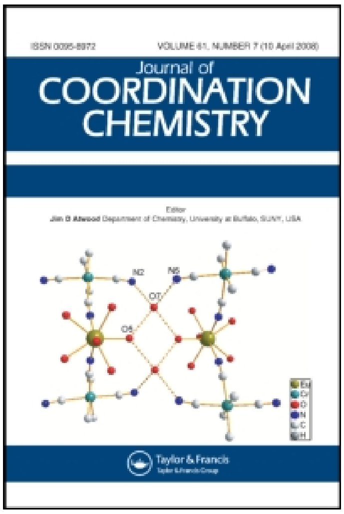

Journal of Coordination Chemistry
Publication details, including instructions for authors and subscription information:
http://www.informaworld.com/smpp/title~content=t713455674

Metal complexes of azo coumarin derivative: synthesis, spectroscopic, thermal, and antimicrobial studies

Samir Alghool[a]
[a] Department of Chemistry, Faculty of Science, Port Said University, Port Said, Egypt

To cite this Article Alghool, Samir(2010) 'Metal complexes of azo coumarin derivative: synthesis, spectroscopic, thermal, and antimicrobial studies', Journal of Coordination Chemistry, 63: 18, 3322 — 3333, First published on: 09 August 2010 (iFirst)

To link to this Article: DOI: 10.1080/00958972.2010.508519

URL: http://dx.doi.org/10.1080/00958972.2010.508519

Journal of Coordination Chemistry
Vol. 63, No. 18, 20 September 2010, 3322–3333

Taylor & Francis
Taylor & Francis Group

Metal complexes of azo coumarin derivative: synthesis, spectroscopic, thermal, and antimicrobial studies

SAMIR ALGHOOL*

Department of Chemistry, Faculty of Science, Port Said University, Port Said, Egypt

(*Received 10 December 2009; in final form 11 May 2010*)

Cu(II), Co(II), Ni(II), Cd(II), and Zn(II) complexes of 6-(2-phenyldiazenyl)-7-hydroxy-4-methyl coumarin (PAHC) are characterized based on elemental analyses, infrared, ^{1}H NMR, magnetic moment, molar conductance, mass spectra, UV-Vis analysis, thermogravimetric analysis (TGA), and X-ray powder diffraction. From the elemental analyses, it is found that the complexes have formulae $[M(L)_2(H_2O)_n]\cdot xH_2O$ (where $M = Cu(II)$, Co(II), Ni(II), Cd(II), and Zn(II), $n = 0–2$, $x = 1–4$). The molar conductance data reveal that all the metal chelates are non-electrolytes. From the magnetic and solid reflectance spectra, it is found that the structures of these complexes are octahedral or tetrahedral. The synthesized ligand and metal complexes were screened for antibacterial activity against some Gram-positive and Gram-negative bacteria.

Keywords: Coumarin; Metal complexes; Bacterial

1. Introduction

Coumarins, both naturally occurring and synthetic derivatives, have found widespread applications as anticoagulant, spasmolytic, and bacteriostatic agents [1–4] and represent an important group of organic compounds used as antibiotics [5, 6], fungicides [7], anti-inflammatory [8], anticoagulant [9], and antitumor agents [10–13].

While coumarin is colorless, some of its derivatives exhibit color and intense fluorescence [14]. Such coumarins have been reported to be useful in solar energy and lasers [15]. The presence of perfluoroalkyl groups in coumarin dyes causes an increase in their photostability and creates bathochromic shifts [16]. The application of coumarin dyes to polyester fabrics gave greenish-yellow to orange shades [17]. A number of coumarins have been investigated for complexing ability [18, 19]. A recent review summarizes advances in the field of cytotoxic properties of coumarins and their coordination complexes [20]. Different coordination compounds and the mechanism of cytotoxic action have been discussed with regard to the development of new antitumor agents. A broad array of medicinal applications of metal complexes of coumarins has been investigated. In some cases the metal complexes obtained had higher biological activity than their ligands [12–23]. In this study new azo dyes were synthesized by

---

*Email: alghools@yahoo.com; samalph2020@yahoo.com

ISSN 0095-8972 print/ISSN 1029-0389 online
DOI: 10.1080/00958972.2010.508519

coupling 7-hydroxy-4-methyl coumarin with diazonium salts, obtained by diazotization of aniline, which is an efficient route for the synthesis of new Cu(II), Co(II), Ni(II), Cd(II), and Zn(II) complexes. Thermal decomposition of their complexes is used to infer the structure. The biological activity of this ligand and metal complexes are evaluated.

2. Experimental

2.1. *Materials and methods*

Purifying and drying of compounds and solvents were performed according to common procedure. Liquid and solid aromatic amines were purified by distillation and recrystallization, respectively. $CuCl_2 \cdot 4H_2O$, $CoCl_2 \cdot 6H_2O$, $NiCl_2 \cdot 6H_2O$, $ZnCl_2 \cdot 6H_2O$, $CdCl_2 \cdot 2H_2O$, and other chemicals were purchased from Fluka and Merck companies, and were used without purification.

2.2. *Analysis*

Elemental analyses (C, H, and N) were performed using a Perkin-Elmer CHN 2400 elemental analyzer. The content of metal ions was calculated gravimetrically as metal oxides. Molar conductance measurements of the ligand and their complexes with $1.0 \times 10^{-3}\,\mathrm{mol\,L^{-1}}$ in DMSO were carried out using a Jenway 4010 conductivity meter. Magnetic measurements were carried out on a Sherwood Scientific magnetic balance using the Gouy method. ^{1}H-NMR spectra from a Varian 200 MHz spectrometer using DMSO as solvent are given as chemical shifts in ppm relative to tetramethylsilane. Electron impact mass spectra were recorded on a Jeol, JMS, DX-303 mass spectrometer. The UV-Vis spectra were obtained in DMSO ($1.0 \times 10^{-3}\,\mathrm{mol\,L^{-1}}$) for the ligand and metal complexes with a Jenway 6405 Spectrophotometer using 1 cm quartz cell from 200 to 600 nm. Infrared (IR) spectra (4000–400 $\mathrm{cm^{-1}}$) were recorded as KBr pellets on a Bruker FT-IR Spectrophotometer. Thermogravimetric analyses (TGA; TG/DTG) were carried out from 25 to 800°C in a steam of nitrogen using Shimadzu TGA 50H TGA. The experimental conditions were: platinum crucible, nitrogen atmosphere with a $30\,\mathrm{mL\,min^{-1}}$ flow rate, and a heating rate of $10^{\circ}\mathrm{C\,min^{-1}}$. X-ray powder diffraction analyses were carried out using a Rigku Model ROTAFLEX Ru-200. Radiation was provided by copper target (Cu anode 2000 W) high-intensity X-ray tube operated at 40 kV and 35 mA. Divergence slit and receiving slit were 1 and 0.1, respectively. The scanning electron microscope (SEM) images were taken in Jeol-840 equipment with an accelerating voltage of 15 kV.

2.3. *Microbiological investigations*

For these investigations the filter paper disc method was applied according to Gupta *et al.* [24]. The investigated bacteria were seeded in tubes with nutrient broth (NB). The seeded NB ($1\,\mathrm{cm^3}$) was homogenized in the tubes with $9\,\mathrm{cm^3}$ of melted (45°C) nutrient agar (NA). The homogeneous suspensions were poured into Petri dishes.

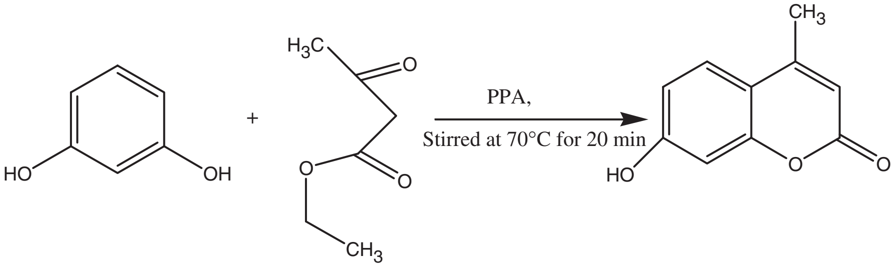

Scheme 1. Preparation of 7-hydroxy-4-methyl coumarin.

Discs of filter paper (diameter 4 mm) were arranged on the cool medium. After cooling the formed solid medium, $2 \times 10^{-5}\,\mathrm{dm}^3$ of the investigated compounds were applied using a micropipette. After incubation for 24 h at 25–27°C, the inhibition (sterile) zone diameters (including disc) were measured and expressed in millimeter. An inhibition zone diameter over 7 mm indicates that the tested compound is active against the bacteria under investigation. The antibacterial activities of the investigated compounds were tested against *Escherichia coli*, *Pseudomonas aeruginosa* as Gram negative, *Bacillus subtilis* and *Staphylococcus aureus* as Gram positive. The concentration of each solution was $1.0 \times 10^{-3}\,\mathrm{mol\,dm}^3$. Commercial DMF was employed to dissolve the tested samples.

2.4. *Synthesis of the ligand*

The preparation of 6-(2-phenyldiazenyl)-7-hydroxy-4-methyl coumarin) (PHM) involves the following two steps.

2.4.1. Preparation of 7-hydroxy-4-methyl coumarin. A mixture of polyphosphoric acid (160 g, obtained by dissolving 126 g of P_2O_5 in 70 g of orthophosphoric acid), resorcinol (11 g, 0.1 mol), and ethylacetoacetate (13 g, 0.1 mol) was stirred and heated at 75–80°C for 20 min (scheme 1). It is poured into ice water and the solid separated was filtered, washed with cold water, and recrystallized from dilute ethanol [25]. Yield: 97%, m.p.: 184°C.

2.4.2. Preparation of azo dyes. To an ice-cooled stirred solution of aromatic amine (10 mmol) in HCl (6 N, 25–30 mL) a cold solution of $NaNO_2$ (7 mL, 10 wt%) was added during 15 min and the reaction mixture was stirred for 45 min at the same temperature. Finally, excess HNO_2 was eliminated by adding solid urea (0.5 g). To a vigorously stirred cold (0–5°C) solution of diazonium salt, a solution of 7-hydroxy-4-methyl coumarin (10 mmol) dissolved in 10 wt% aqueous solution of NaOH (15 mL) was added. After stirring for 30 min, the mixture was neutralized by adding HCl (15 mL, 10 wt%). The obtained precipitate was isolated by filtration and washed with water and cold ethanol. The crude dye was purified by recrystallization.

2.5. *Synthesis of metal complexes*

All Cu(II), Co(II), Ni(II), Cd(II), and Zn(II) complexes were synthesized by adding appropriate metal chlorides (1.0 mmol, in 20 mL ethyl alcohol : water (50 : 50) volume to a hot solution of ligand (2.0 mmol, in 30 mL ethyl alcohol (95%)). The resulting solutions were stirred and refluxed on a hot plate at 80°C for 3 h and the colored solid formed was filtered, washed with ethanol and diethyl ether, and finally dried under vacuum. All complexes were prepared and isolated as amorphous solids.

3. Results and discussion

The azo dye of coumarin was prepared by coupling 7-hydroxy-4-methyl coumarin with diazotized aniline. Selected physical properties and characteristic data of the synthesized dye and metal complexes are listed in table 1. All the complexes show 1 : 2 metal : ligand stoichiometry. The isolated solid complexes are stable in air and insoluble in water or ethyl alcohol, but soluble in DMF and DMSO. Molar conductance indicates that all the complexes are nonelectrolytes. The ligand was decomposed at temperatures higher than 200°C. Elemental analyses were in good agreement with those required for the formulas.

3.1. *Mass spectra*

Mass spectra of 6-(2-phenyldiazenyl)-7-hydroxy-4-methyl coumarin shown in Supplementary material confirm the proposed formula with the appearance of a peak at 280 amu ($C_{12}H_{11}O_2N_3S$, calculated atomic mass 280 amu) and other peaks at 77, 92, 105, 147, 189, and 203 amu due to different fragments.

3.2. *Molar conductance measurements*

The molar conductivities for the coumarin azo dye complexes in DMSO (10^{-3} mol dm^{-3}) were in the range 14–22 Ω^{-1} cm^2 mol^{-1}, suggesting them to be nonelectrolytes (table 1). This was confirmed from the chemical analysis (elemental analysis data), where Cl^- are not precipitated by the addition of $AgNO_3$.

3.3. *UV-Vis spectra and magnetic measurements*

UV-Vis spectra of the ligand and its metal complexes are recorded in DMF from 200 to 800 nm. The ligand shows three bands at 215, 317, and 355 nm, which may be attributed to π–π^*, π–π^*, and n–π^* transitions. These bands are shifted to 221–236, 301–307, and 360–368 nm, respectively, upon coordination.

The electronic spectral data of the Cu complex, $[Cu(PAHC)_2]\cdot H_2O$, gave d–d transition at 584 nm assigned to the transition $^2E \rightarrow {}^2T_2$. Its magnetic moment $\mu_{eff} = 1.73$ B.M. is very close to tetrahedral geometry. Electronic spectra of Co complex, $[Co(PAHC)_2(H_2O)_2]\cdot 2H_2O$, gave visible d–d electronic spectral bands at 454, 575,

Table 1. Elemental analyses and physical data of PAHC and complexes.

								Elemental analyses (Calcd (found))			
Compounds	Empirical formula	M.wt	Ω^{-1} (cm^2 mol^{-1})	Color	m.p.	Yield	μ_{eff}	%C	%H	%N	%M
PAHC	$C_{16}H_{12}O_3N_2$	280.08	14	Red	186	90	–	68.56(68.17)	4.32(4.44)	9.99(9.87)	
$[Cu(PAHC)_2] \cdot H_2O$	$C_{32}H_{24}O_7N_4Cu$	639.09	18	Dark red	>300	88	1.52	60.04(60.22)	3.78(3.59)	8.75(8.97)	9.93(10.26)
$[Co(PAHC)_2(H_2O)_2] \cdot 2H_2O$	$C_{32}H_{30}O_{10}N_4Co$	689.13	16	Brown	>300	87	5.12	55.74(55.88)	4.39(4.21)	8.13(8.47)	8.55(8.00)
$[Ni(PAHC)_2(H_2O)_2] \cdot 2H_2O$	$C_{32}H_{30}O_{10}N_4Ni$	688.13	18	Brown	>300	77	3.26	55.76(55.45)	4.39(4.32)	8.13(8.26)	8.51(7.99)
$[Cd(PAHC)_2(H_2O)_2] \cdot 4H_2O$	$C_{32}H_{28}O_9N_4Cd$	726.09	16	Dark red	234	82	–	49.34(49.63)	4.40(4.71)	7.19(7.47)	14.43(14.12)
$[Zn(PAHC)_2] \cdot 2H_2O$	$C_{32}H_{26}O_8N_4Zn$	658.10	14	Dark red	>300	78	–	58.24(58.81)	3.97(3.68)	8.49(8.23)	9.91(9.27)

and 641 nm assigned to ${}^4T_{1g}(F) \rightarrow {}^4T_{2g}(P)$, ${}^4T_{1g}(F) \rightarrow {}^4A_{2g}(F)$, ${}^4T_{1g}(F) \rightarrow {}^4T_{2g}(F)$, and its effective room temperature magnetic moment $\mu_{eff} = 5.12$ B.M. is typical of high spin octahedral [26, 27]. The $[Ni(PAHC)_2(H_2O)_2] \cdot 2H_2O$ complex showed d–d electronic bands at 497, 571, and 640 nm assigned to ${}^3A_{2g} \rightarrow {}^3T_{1g}(P)$, ${}^3A_{2g} \rightarrow {}^3T_{1g}(F)$, ${}^3A_{2g} \rightarrow {}^3T_{2g}$. The $\mu_{eff} = 3.26$ B.M. supported the existence of octahedral geometry [28–33]. $[Cd(PAHC)_2(H_2O)_2] \cdot H_2O$ and $[Zn(PAHC)_2] \cdot 2H_2O$ complexes are diamagnetic as expected.

3.4. *IR spectra and mode of bonding*

The IR spectral bands of the ligand and complexes are listed in table 2 together with assignments. The functional groups of the azo-linked ligand and the metal complexes have been detected by IR spectra (Supplementary material).

A comparison of IR spectra of the ligand and complexes reveals the disappearance of absorptions associated with OH stretch of the phenol, indicating loss of phenolic proton on complexation, forming a metal–oxygen bond. This was further supported by the decrease in ν(C–O) frequency by 8–36 cm^{-1} [34].

Bands at 1602 cm^{-1} were assigned to the stretching vibration of the azo of PAHC [35], which shifted in the complexes by *ca* ~20 cm^{-1} to lower wavenumber because of nitrogen coordination, withdrawing electrons from nitrogen.

IR spectra of the complexes have a broad band at 3421–3438 cm^{-1} attributed to OH of crystal water [36], while $\nu(H_2O)$ of coordinated water appear at 837–844 cm^{-1} [37]. In the far IR spectra of all the complexes, non-ligand bands at 510–523 and 410–459 cm^{-1} can be assigned to ν(M–O) and ν(M–N), respectively [38, 39]. Therefore, the IR spectra reveal that PAHC coordinates to metals *via* azo-N and phenolic-O of coumarin.

3.5. *^{1}H NMR spectra*

Proton spectra of the compounds recorded at 250 MHz in DMSO-d$_6$ confirm the formation of the complex; typical chemical shifts of the ^{1}H NMR spectra in DMSO-d$_6$ are summarized in "Supplementary material". Different chemical shifts in the Zn(II) complex were attributed to coordination. Comparison of the ^{1}H NMR spectra of the complex with the ligand reveals that the resonances are considerably broadened and also shifted on complexation. The ^{1}H NMR spectrum of the ligand shows a singlet at 2.4 ppm due to $-CH_3$ group, phenyl rings at $\delta = 6.8$–8.4 ppm, and a broad signal near 14.2–14.4 ppm, indicating a NH resonance of the hydrazone (scheme 2 in Supplementary material). In the ^{1}H NMR spectrum of Zn(II) complex, the $-CH_3$ is at 2.2 ppm and aromatic protons at 6.9–9.00 ppm. Disappearance of the broad signal at 14.2–14.4 ppm indicates that coordination takes place through nitrogen of azo.

3.6. *Thermogravimetric analysis*

Thermal properties of Cu(II), Co(II), Ni(II), Cd(II) and Zn(II) complexes are summarized in Supplementary material. The data from TGA clearly indicate that

Table 2. IR spectral data of PAHC and Cu(II), Co(II), Ni(II), Cd(II), and Zn(II) complexes (cm^{-1}).

Compounds	ν(OH) hydrated	ν(OH) Coord.	ν(C=O)	ν(OH) phenolic	ν(C–O) phenolic	N=N	ν(M–O)	ν(M–N)
PAHC	–	–	1720(s)	3386(br)	1284(m)	1602	–	–
$[Cu(PAHC)_2]$	3421(br)	–	1725(s)	–	1256(m)	1583(s)	511(s)	447(m)
$[Co(PAHC)_2(H_2O)_2] \cdot 2H_2O$	3438(br)	837(m)	1718(s)	–	1260(w)	1580(s)	516(m)	459(w)
$[Ni(PAHC)_2(H_2O)_2] \cdot 2H_2O$	3438(br)	842(w)	1706(m)	–	1253(w)	1579(s)	520(w)	451(w)
$[Cd(PAHC)_2(H_2O)_2] \cdot 4H_2O$	3423(br)	838(m)	1722(s)	–	1238(m)	1585(s)	523(m)	439(m)
$[Zn(PAHC)_2] \cdot 2H_2O$	3426(br)	844(m)	1714(m)	–	1276(m)	1594(s)	510(m)	410(w)

br = broad; s = strong; w = weak; m = medium.

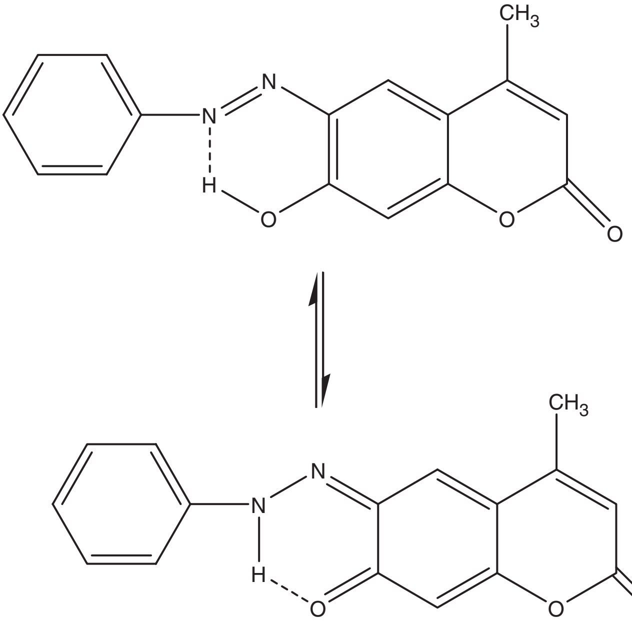

Scheme 2. Resonance of the hydrazone form.

decomposition of the complexes proceeds in three or four steps (table 3). Crystal water molecules were lost between 25 and 160°C and coordinated water between 160 and 250°C. The decomposition of all complexes ended with the metal or stoichiometric oxide formation and carbon residue.

3.6.1. Thermal properties of $[Cu(PAHC)_2]\cdot H_2O$. $[Cu(PAHC)_2]\cdot H_2O$ gives three stages of decomposition. The first stage, 25–120°C, represents loss of one hydrated water molecule. The temperature range 280–385°C corresponds to the loss of organic molecules. The final products, formed above 700°C, consist of copper oxide and carbon residue.

3.6.2. Thermal properties of $[Co(PAHC)_2(H_2O)_2]\cdot 2H_2O$ and $[Ni(PAHC)_2(H_2O)_2]\cdot 2H_2O$ complexes. The TGA of $[Co(PAHC)_2(H_2O)_2]\cdot 2H_2O$ and $[Ni(PAHC)_2(H_2O)_2]\cdot 2H_2O$ give four stages. The first at 25–120°C represents loss of two crystal water molecules, the second at 120–200°C represents loss of two coordinated water molecules. The final decomposition products are metal oxide and carbon residue.

3.6.3. Thermal properties of $[Cd(PAHC)_2(H_2O)_2]\cdot 4H_2O$ and $[Zn(PAHC)_2]\cdot 2H_2O$ complexes. Thermal decompositions of $[Cd(PAHC)_2(H_2O)_2]\cdot 4H_2O$ and $[Zn(PAHC)_2]\cdot 2H_2O$ are in three or four decomposition steps. The first stage, at 40–140°C, is from loss of four crystal water molecules for Cd(II) and two for Zn(II). The second stage for Cd(II) at 140–200°C corresponds to loss of two coordinated water molecules; Zn(II) shows no weight loss for coordinated water. From 250°C to 450°C,

Table 3. Thermal data of PAHC and metal complexes.

Compounds	Temperature range (°C)	DTG peak (°C)	TG Weight loss (%) Calcd/Found	Assignments
$[Cu(PAHC)_2]$	25–120	77	2.81(3.11)	H_2O
	120–600	465	75.44(75.82)	Organic moiety
	>600		21.75(21.07)	$CuO + 5C$
$[Co(PAHC)_2(H_2O)_2] \cdot 2H_2O$	25–120	75	5.22(5.43)	$2H_2O$
	120–200	180	5.22(5.55)	$2H_2O$
	200–600	371	68.67(67.41)	Organic moiety
	>600		20.89(21.61)	$1/2(Co_2O_3) + 5C$
$[Ni(PAHC)_2(H_2O)_2] \cdot 2H_2O$	25–120	75	5.23(5.28)	$2H_2O$
	120–200	174	5.23(5.65)	$2H_2O$
	200–600	384	69.92(70.11)	Organic moiety
	>600		19.62(18.96)	$NiO + 5C$
$[Cd(PAHC)_2(H_2O)_2] \cdot 4H_2O$	25–140	80	9.91(10.00)	$4H_2O$
	140–200	160	4.95(4.81)	$2H_2O$
	200–600	377	69.44(68.93)	Organic moiety
	>600		15.70(16.26)	Cd
$[Zn(PAHC)_2] \cdot 2H_2O$	25–120	70	5.47(5.58)	$2H_2O$
	120–600	380	77.06(76.55)	Organic moiety
	>600		17.47(17.87)	$ZnO + 3C$

$$[M(L)_2(H_2O)_n]\cdot mH_2O \xrightarrow[\text{Dehydration}]{25\text{–}140^\circ C} [M(L)_2(H_2O)_n] + mH_2O$$

$$[M(L)_2(H_2O)_n] \xrightarrow{140\text{–}400^\circ C} [M(L)_2] + nH_2O$$

$$[M(L)_2] \xrightarrow[\text{Final decomposition}]{400\text{–}700^\circ C} \text{Metal oxide + L+ carbon residue}$$

M=Cu, Co, Ni, Cd or Zn; L=PAHC; n=0 or 2; m=1, 2 or 4

Scheme 3. Thermal degradation steps of PAHC ligand and their metal complexes.

organic part is lost. The final products, formed above 700°C, consist of Cd metal and zinc oxide and carbon residue.

In general, the stages of thermal decomposition of the complexes can be written as in scheme 3.

3.7. *X-ray powder diffraction*

Single crystals of the complexes could not be isolated; however, the spectroscopic data and elemental analyses enable us to predict structures.

X-ray powder diffraction patterns in the $5^\circ < 2\theta < 90^\circ$ were carried out in order to obtain lattice dynamics of the compound. The obtained X-ray powder diffraction patterns are shown in the "Supplementary material". This identification of the complexes was done by the known method [40] and suggests that the prepared compounds are amorphous.

Table 4. Antibacterial activity data of PAHC and metal complexes, inhibition zone (mm).

Compounds	*Bacillus subtili* G^+	*Staphylococcus aureus* G^+	*Escherichia coli* G^-	*Pseudomonas aeruginosa* G^-
PAHC	18	18	18	17
$[Cu(PAHC)_2]$	20	16	17	18
$[Co(PAHC)_2(H_2O)_2] \cdot 2H_2O$	26	23	24	24
$[Ni(PAHC)_2(H_2O)_2] \cdot 2H_2O$	24	26	26	22
$[Cd(PAHC)_2(H_2O)_2] \cdot 4H_2O$	24	21	26	21
$[Zn(PAHC)_2] \cdot 2H_2O$	20	24	23	23
Norfloxacin	18	19	17	17
Control (DMSO)	0	0	0	0

Less than 10 mm = inactive, 10–15 mm = weakly active, 15–20 mm = moderately active; more than 20 mm = highly active (error limits 1–2 mm).

3.8. *Microbiological investigation*

Biological activities of the azo coumarin ligand and metal complexes were tested against bacteria. The organisms used in the present investigation include two Gram-positive bacteria (*B. subtillis* and *S. aureus*) and two Gram-negative bacteria (*E. coli* and *P. aereuguinosa*). Norfloxacin was used as the standard against respective bacteria. DMSO was used as the control. The concentration of DMSO used for testing was $1\,mg\,mL^{-1}$, whereas Norfloxacin solution was $1.0 \times 10^{-3}\,mol\,dm^{-1}$. The antimicrobial activity was estimated on the basis inhibition zone. The results of the bactericidal screening of the synthesized compounds are recorded in table 4. The complexes have enhanced activity compared to the azo coumarin ligand itself (Supplementary material). The ligands and their complexes have high activity toward *Bacillus subtili* (G^+) in the order $[Co(PAHC)_2(H_2O)_2] \cdot 2H_2O > [Ni(PAHC)_2(H_2O)_2] \cdot 2H_2O = [Cd(PAHC)_2(H_2O)_2] \cdot H_2O > [Zn(PAHC)_2] \cdot 2H_2O = [Cu(PAHC)_2] >$ PAHC > Norfloxacin. In the case of *Escherichia coli* (G^-), $[Ni(PAHC)_2(H_2O)_2] \cdot 2H_2O = [Cd(PAHC)_2(H_2O)_2] \cdot H_2O > [Co(PAHC)_2(H_2O)_2] \cdot 2H_2O > [Zn(PAHC)_2] \cdot 2H_2O >$ PAHC $> [Cu(PAHC)_2] =$ Norfloxacin.

3.9. *Structure of complexes*

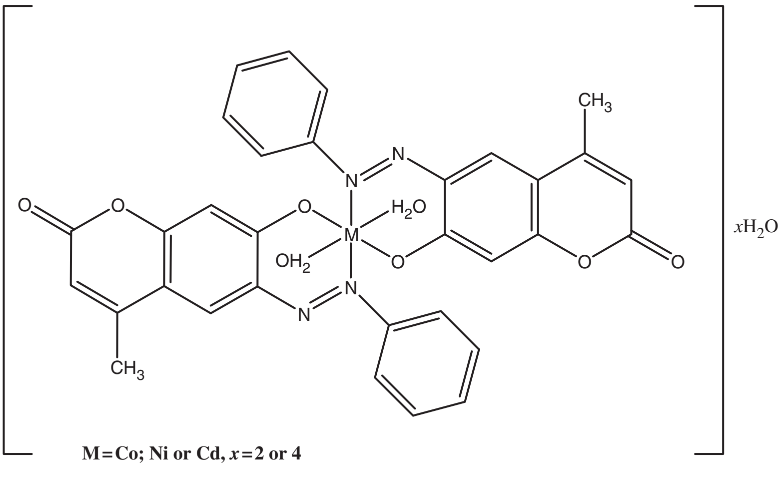

M = Co; Ni or Cd, x = 2 or 4

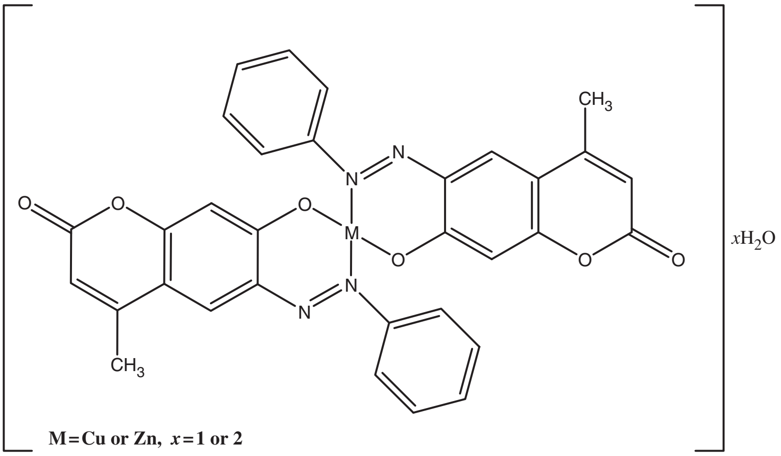

4. Conclusion

The coordination ability of 6-(2-phenyldiazenyl)-7-hydroxy-4-methyl coumarin has been proved in complexation with Cu(II), Co(II), Ni(II), Cd(II), and Zn(II). The elemental analysis and TGA confirmed the compositions of the compounds. ^{1}H NMR, IR, UV-Vis spectra and magnetic measurements of the ligand and metal complexes confirmed the suggested coordination of the ligands through azo-N and phenolic-O of coumarin. Under experimental conditions employed, only 1 : 2 (M : L) complexes have been found.

References

[1] H.B. Singh. *Acta Cienc. Indica, [Ser.] Chem.*, **6**, 88 (1980).
[2] G. Luzzatto, F. Fabris, R. DalBo Zanon, A. Giralami. *Arzneim. Forsch.*, **36**, 972 (1986).
[3] J. Baskaran, R. Kanakasabai, P. Neelanarayanan. *Ind. J. Exp. Biol.*, **33**, 113 (1995).
[4] L.E. Twigg, B.J. Kay. *Comp. Biochem. Physiol. Pharmacol. Toxicol. Endocrinol.*, **110**, 77 (1995).
[5] A. Maxwell. *Mol. Microbiol.*, **9**, 681 (1993).
[6] O.A. Abd-Allah. *Farmaco*, **55**, 641 (2000).
[7] A.M. El-Agrody, M.S.A. El-Latif, N.A. El-Hady, A.H. Fakary, A.H. Bedair. *Molecules*, **6**, 519 (2001).
[8] A.A. Emmanuel-Giota, K.C. Fylaktakidou, D.J. Hadjipavlou-Litina, K.E. Litinas, D.N. Nicolaides. *J. Heterocycl. Chem.*, **38**, 717 (2001).
[9] I. Manolov, N.D. Danchev. *Eur. J. Med. Chem.*, **30**, 531 (1995).
[10] F.H. Dexeus, C.J. Logothetis, A. Sella, K. Fitz, R. Amato, J.M. Reuben, N.J. Dozier. *J. Clin. Oncol.*, **8**, 325 (1990).
[11] Z.M. Nofal, M.I. El-Zahar, S.S. El-Karim. *Molecules*, **5**, 99 (2000).
[12] H. Madari, D. Panda, L. Wilson, R. Jacobs. *Cancer Res.*, **63**, 1214 (2003).
[13] D. Conley, E.M. Marshall. *Proc. Am. Assoc. Cancer Res.*, **28**, 63 (1987).
[14] N.R. Ayyangar, K.V. Srinivasan, T. Daniel. *Dyes Pigm.*, **13**, 301 (1990).
[15] N.R. Ayyangar, K.V. Srinivasan, T. Daniel. *Dyes Pigm.*, **16**, 197 (1991).
[16] M. Matsui. *J. Flourine Chem.*, **96**, 65 (1999).
[17] A.S. Shawali, I.F. Zeid, M.H. Abdelkader, A. Alsayed Elsherbini, F.M.A. Altalbawy. *J. Chin. Chem. Soc.*, **48**, 65 (2001).
[18] A.U. Mandakmare, M.L. Navwade. *Orient. J. Chem.*, **13**, 155 (1997).
[19] A.L. El-Ansary, M.M. Omar. *Egypt. J. Chem.*, **31**, 511 (1988).
[20] I. Kostova. *Curr. Med. Chem. Anticancer Agents*, **5**, 29 (2005).

[21] I. Kostova, I. Manolov, M. Karaivanova. *Arch. Pharm. Pharm. Med. Chem.*, **334**, 157 (2001).
[22] I. Kostova, I. Manolov, I. Nicolova, N. Danchev. *Il Farmaco*, **56**, 707 (2001).
[23] I. Kostova, R. Kostova, G. Momekov, N. Trendafilova, M. Karaivanova. *J. Trace Elem. Med. Biol.*, **18**, 219 (2005).
[24] R. Gupta, R.K. Saxena, P. Chatarvedi, J.S. Virdi. *J. Appl. Bacteriol.*, **78**, 378 (1995).
[25] V.K. Ahluwalia, R. Aggarwal. *Comprehensive Practical Organic Chemistry, Preparation and Quantitative Analysis*, Universities Press (India) Limited, Hyderabad, India (2000).
[26] C. Paen, G. Tosi. *Aust. J. Chem.*, **29**, 543 (1976).
[27] N. Mondal, D.K. Dey, S. Mitra, K.M. Abdul Malik. *Polyhedron*, **19**, 2707 (2000).
[28] D.R. Zhu, Y. Song, Y. Xu, Y. Zhang, S.S.S. Raj, H.K. Fun, X.Z. You. *Polyhedron*, **19**, 2019 (2000).
[29] F.A. Cotton, G. Wilkinson, C.A. Murillo, M. Bochmann. *Advanced Inorganic Chemistry*, 6th Edn, Wiley, New York (1999).
[30] S. Chandra, A. Kumar. *Spectrochim. Acta, Part A*, **68**, 469 (2007).
[31] C.M. Sharaby. *Spectrochim. Acta, Part A*, **62**, 326 (2005).
[32] A.I. Vogel. *Quantitative Inorganic Analysis Including Elemental Instrumental Analysis*, 2nd Edn, Longmans, London (1962).
[33] C. Sulekh, K.B. Londeya, R.P. Singh. *J. Ind. Chem. Soc.*, 8 (1981).
[34] P. Venkateswara Rao, N. Rama Rao, M.C. Ganorkar. *Indian J. Chem.*, **27A**, 160 (1988).
[35] M.S. Refat, I.M. El-Deen, H.K. Ibrahim, S. El-Ghool. *Spectrochim. Acta, Part A*, **65**, 1208 (2006).
[36] S. Shirctake. *Chem. Pharm. Bull.*, **28**, 1673 (1980).
[37] M.S. Masoud, H.M. El-Nahas, S.S. Haggag. *Pak. J. Sci. Ind. Res.*, **38**, 108 (1998).
[38] L. Casella, M. Gullotti. *J. Am. Chem. Soc.*, **103**, 6338 (1981).
[39] J.R. Ferraro. *Low Frequency Vibrations of Inorganic and Coordination Compounds*, 1st Edn, p. 168, Plenum Press, New York (1971).
[40] B.D. Cullity. *Elements of X-ray Diffraction*, 2nd Edn, Addison-Wesley Inc., Reading, MA (1993).